Research Article | Vol. 28, No. 25 / 7 December 2020 / Optics Express 37903

Optics EXPRESS

Broadband, few-cycle mid-infrared continuum based on the intra-pulse difference frequency generation with BGSe crystals

JINWEI ZHANG,[1,2,6,*] QING WANG,[3,6] JINGJIE HAO,[1] HEYAN LIU,[1] JIYONG YAO,[4] ZHUANG LI,[4] JIE LIU,[5] AND KA FAI MAK[2]

[1] *School of Optical and Electronic Information and Wuhan National Laboratory for Optoelectronics, Huazhong University of Science and Technology, Wuhan 430074, China*
[2] *Max-Planck Institute of Quantum Optics, Hans-Kopfermann-Str. 1, 85748 Garching, Germany*
[3] *School of Optics and Photonics, Beijing Institute of Technology, Beijing 100081, China*
[4] *Beijing Center for Crystal Research and Development, Key Lab of Functional Crystals and Laser Technology, Technical Institute of Physics and Chemistry, Chinese Academy of Sciences, Beijing 100190, China*
[5] *School of Physics and Electronics, Shandong Normal University, Jinan 250358, China*
[6] *These authors contributed equally to the manuscript.*
[*] *jinweizhang@hust.edu.cn*

Abstract: We demonstrate for the first time the generation of octave-spanning mid-infrared using a BGSe nonlinear crystal. A Cr:ZnS laser system delivering 28-fs pulses at a central wavelength of 2.4 µm is used as the pump source, which drives the intra-pulse difference frequency generation inside the BGSe crystal. As a result, a coherent broadband mid-infrared continuum spanning from 6 to 18 µm has been obtained. It shows that the BGSe crystal is a promising material for broadband, few-cycle mid-infrared generation via frequency down conversion with femtosecond pump sources.

1. Introduction

Mid-infrared (MIR) light in the range of 2-20 µm is useful for chemical and biological identification due to the presence of many molecular characteristic absorption lines in this spectral region [1]. A coherent, few-cycle source with a simultaneous coverage of the broad MIR range can further enable new applications such as mirco-spectroscopy [2,3], femtosecond pump-probe spectroscopy [4], and high-dynamic-range sensitive measurements [5–7] Until now numerous schemes have been developed to generate coherent MIR radiation, such as synchrotron beam lines, quantum cascade lasers, supercontinuum sources [2], optical parametric oscillators (OPO) [8] and optical parametric amplifiers (OPA). These schemes all have their own strengths and weaknesses in terms of complexity, bandwidth, power, efficiency, and pulse durations. Among them, intra-pulse difference frequency generation (IDFG) is attracting growing attention thanks to the development of high-power femtosecond 2 µm lasers that can effectively pump small-bandgap non-oxide nonlinear crystals to generate high-power broadband coherent MIR light [9–13]. Compared to the normally used OPOs and OPAs, IDFG allows a reduction in system complexity and enhancement of reliability, as the need to align two separate beams or cavities at high precision is removed. Besides, the MIR output is intrinsically carrier-envelope-phase (CEP) stable with IDFG [7].

For the purpose of broadband coherent MIR generation with IDFG, suitable nonlinear media with a wide transparency range, large nonlinear coefficient and high damage threshold are called for. A number of nonlinear crystals have been successfully utilized to generate coherent broadband MIR by IDFG, including $LiGaS_2$ (LGS) [14], GaSe [9–13,15], ZGP [11,16], and ZnSe/ZnS [17]. The parameters of these MIR sources are summarized in Table 1. Yet the exploration of new nonlinear crystals for MIR generation is far from complete. In 2010, a new biaxial chalcogenide

#411664 https://doi.org/10.1364/OE.411664
Journal © 2020 Received 5 Oct 2020; revised 18 Nov 2020; accepted 19 Nov 2020; published 1 Dec 2020

nonlinear crystal, $BaGa_4Se_7$ (BGSe), has been fabricated using the Bridgman-Stockbarger method [18,19]. It has a wide transparency range from 0.47 to 18 µm (as shown in Fig. 1) with nonlinear coefficients of $d_{11} = 24.3$ pm/V and $d_{13} = 20.4$ pm/V. The transparency window of BGSe is significantly broader than ZGP and LGS although its nonlinearity is lower than ZGP (75 ± 8 pm/V) [20]. In contrast to GaSe, BGSe can also be cut at the desired phase-matching angle and can be anti-reflection coated. Recently another new chalcogenide nonlinear crystal BGGSe was developed and used for MIR generation [21,22], showing very similar transparency window and higher nonlinear coefficient (d_{11}=66 pm/V) compared to BGSe. However, BGSe crystal can be more easily grown to a large dimensions to accommodate larger beam sizes [19]. These make BGSe a promising nonlinear crystal for high power, broadband MIR generation.

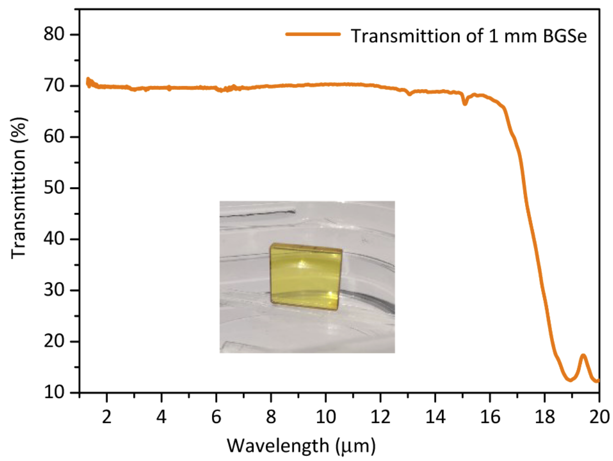

Fig. 1. Transmission spectrum of the 1-mm-thick uncoated BGSe crystal. The inset shows the actual crystal used in this experiment.

Table 1. Summary of the parameters with selected IDFG sources. *NL crystal*, nonlinear crystal; λ_{pump}, pump wavelength; τ, pulse duration of the pump pulses; f_{rep}, repetition rate of the pump pulses; P_{pump}, pump average power; P_{MIR}, average power of the MIR generated by IDFG; λ_{MIR}, spectral span of MIR; η, conversion efficiency.

NL crystal	λ_{pump} [µm]	τ [fs]	f_{rep} [MHz]	P_{pump} [W]	P_{MIR} [mW]	λ_{MIR} [µm]	η [%]	*Ref.*
LGS	1.03	19	100	50	103	6.8-16.4	0.21	[14]
ZnSe	2.09	15	77	7	25	2.7-20	0.36	[17]
ZnS	2.09	15	77	7	35	2.7-15	0.5	[17]
GaSe	2.09	15	77	7	24	4.4-20	0.34	[9]
GaSe	1.95	16	1.25	32	450	6-18	1.41	[12]
GaSe	2.5	20	78	6	13	4.3-16.6	0.22	[11]
ZGP	2.5	20	78	4.5	148	5.8-12.5	3.3	[11]
GaSe	2.4	28	69	3.4	15	2.7-17	0.44	[10]
BGSe	2.4	28	69	1.1	1.9	6-18	0.17	[this work]

Efficient MIR generation has been reported with BGSe crystals in the schemes of OPA, OPO and difference-frequency mixing [23–31]. In all these works, pulses longer than a picosecond were used as the driving sources for the parametric conversion, and a simultaneous coverage of the broad MIR range has not been realized with BGSe crystals. In this work, we demonstrate the generation of a coherent MIR output with a BGSe crystal via IDFG. Driven by femtosecond pulses at 2.4 μm, the resulting spectrum simultaneously covers the range between 6 and 18 μm. This is, to the best of our knowledge, the broadest MIR spectrum generated from frequency down conversion using a BGSe crystal to date. The damage threshold of the BGSe crystal was also characterized under femtosecond pulses with a central wavelength of 2.4 μm.

2. Experimental setup

The experimental setup is illustrated in Fig. 2(a). The driving pulses are initially generated from a home-built Kerr-lens mode-locked Cr:ZnS oscillator [32–36] with a polycrystalline Cr:ZnS crystal ($5 \times 2 \times 9$ mm^3, transmission=15% at 1908nm) as the gain medium pumped by a Tm-doped fiber laser at 1908nm. The oscillation in a standing-wave cavity delivers 45-fs pulses operating at a repetition rate of 69 MHz with an average power of 1 W at a carrier wavelength of 2.4 μm. The power is amplified to 3.3 W in a home-built two-stage single-pass polycrystalline Cr:ZnS amplifier ($5 \times 2 \times 6$ mm^3, transmission=20% at 1908nm and $5 \times 2 \times 9$ mm^3, transmission=15% at 1908nm) [10], and the output pulse duration is measured with a home-built second-harmonic-generation frequency-resolved optical grating (SHG-FROG) apparatus. The retrieved pulse duration, at 28 fs (Fig. 2(c)), corresponds to 3.5 optical cycles of the carrier wave at 2.4 μm. Figure 2(b) shows the spectrum after the amplification stage spanning from 2 to 2.6 μm, which determines the interacting wavelength range through the IDFG process. Compared to pumping at 1 μm, the use of longer pump wavelengths enables the use of highly nonlinear non-oxide crystals with broad mid-IR transparency to achieve the desired broadband phase matching. In addition, a lower photon energy can mitigate multiphoton absorption in the nonlinear crystal, enabling a higher damage threshold of the crystal. Furthermore, the conversion efficiency of IDFG can also be enhanced, as it scales quadratically with the effective interaction length, which lengthens as the pump wavelength increases [11].

The driving pulses were focused by a gold-coated off-axis parabolic mirror into a 1-mm-thick, uncoated BGSe crystal (DIEN TECH) down to a spot diameter of 46 μm. The BGSe crystal is cut at an angle of θ=40.5° and $\varphi = 0°$ for Type I phase matching, as shown in Fig. 3(a). We optimized the phase matching condition by rotating the crystal and a half-wave plate. The generated MIR radiation was separated from the transmitted fundamental driving beam by long-pass filters and then sent to a power meter and a monochromator (Newport Cornerstone 260) for power and spectral measurement, respectively.

The driving power was set as 1.1 W to keep it below the damage threshold. The corresponding peak intensity in the focus was 37.3 GW/cm^2 taking into account the high reflection loss of the uncoated BGSe. The generated MIR was focused by a ZnSe lens into the monochromator for the spectral measurement. To suppress second-order diffractions from the monochromator's grating, three long-pass filters with cut-on wavelengths at 4.5, 7.3, and 11 μm were used, and three different spectra spanning from 4.5 to 8.5 μm, 6 to 13 μm, and 10 to 22 μm were recorded, respectively. A silicon nitride infrared emitter (Bentham Instruments Ltd) was used to calibrate the intensities of the measured spectra and correct for losses in the long-pass filters and the ZnSe lens, and the low diffraction efficiency of the monochromator grating at longer wavelengths (starting from 11 μm). The corrected spectra were then stitched together to obtain the final spectrum.

The measured spectrum shown in Fig. 4(a) covers the wavelength range from 6 to 18 μm (at −30 dB), which can support few-cycle pulses in the MIR. We simulated the spectrum numerically based on the one-dimensional (1D) + time split-step method [37], where spatial effects such as walk-off and self-focusing were not considered. With the measured FROG data of the driving pulses as the input, the output IDFG spectrum was simulated, as shown in Fig. 4(a). The simulated spectrum matches well with the experimental result in the wavelength range of 6-18 μm. The dip in the wavelength around 15 μm in the experimental spectrum results from the absorption lines of carbon dioxide in the beam path to the monochromator, which was not considered in the

Optics EXPRESS

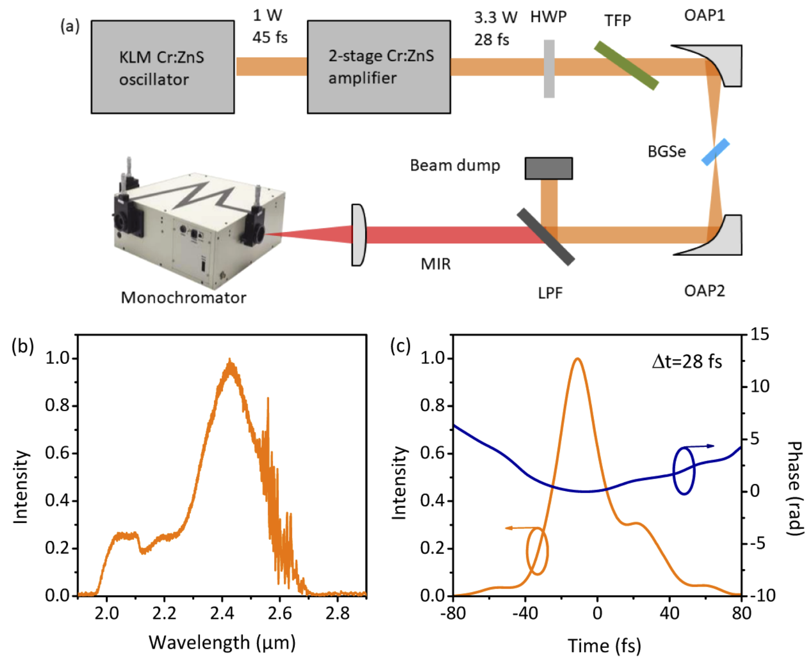

Fig. 2. (a) Experimental setup of the MIR generation with a BGSe crystal. OAP, off-axis parabolic mirror with an effective focus length of 20 mm; HWP, half-wave plate; TFP, thin-film polarizer; LPF, long-pass filter. (b) Measured spectrum of the driving pulses. (c) Corresponding temporal profile retrieved from a SHG-FROG measurement, showing a pulse duration of 28 fs.

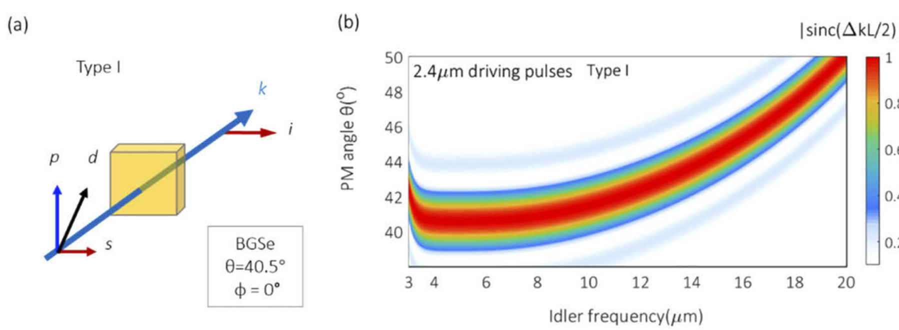

Fig. 3. (a) Type I phase-matching scheme in biaxial BGSe crystals. The arrows indicate polarizations (*d*: driver; *p*: pump; *s*: signal; *i*: idler) and wave vector (*k*). (b) Optimal phase matching angle and phase matching function [sinc ($\Delta kL/2$)] in a BGSe crystal with respect to the generated signal (idler) with a 2.4 µm pump beam.

simulation. Figure 4(b) shows the numerically simulated temporal characteristics of the MIR pulses, and the predicted pulse duration, directly after the crystal, of 42 fs—corresponding to almost one optical cycle for pulses at the carrier wavelength of 11 µm. The Fourier transform limit is even shorter at 29 fs for the simulated spectrum and 22 fs for the experimentally measured spectrum. A pulse duration of less than one optical cycle at the wavelength of 11 µm could therefore be expected if the dispersion of the BGSe crystal and the long-pass filter in the MIR beam path, which amounts to ~-1500 fs^2, can be compensated.

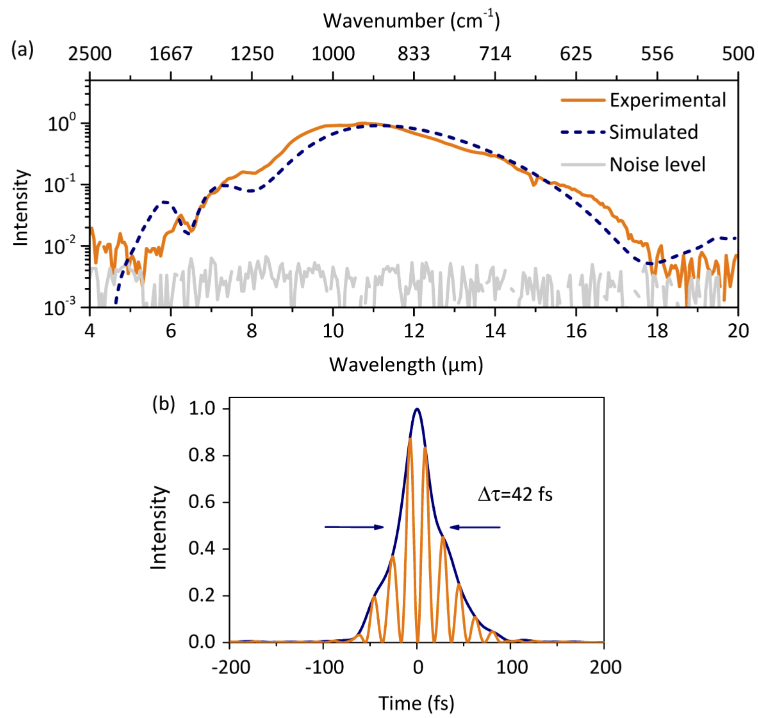

Fig. 4. (a) The experimentally measured and numerically simulated MIR spectrum. (b) Simulated pulse shape (black curve) and absolute electrical field intensity (red curve) of the MIR pulses.

An average power of 1.2 mW was measured (S302C, Thorlabs) behind the long-pass filter with a cut-on wavelength of 4.5 µm. Taking into account the >10% loss of the long-pass filter above 4.5 µm and the reflection loss due to the uncoated BGSe crystal surface, the generated MIR power inside the crystal can be calculated as 1.9 mW, which can already fulfill many applications in field-resolved detection. Further investigation on power scaling, such as by increasing the focus spot size while keeping the intensity the same, could potentially yield even higher output power.

With a band gap of 2.64 eV, BGSe crystal has been reported to have a damage threshold of 100 MW/cm^2 at 1.064 µm and 122.2 MW/cm^2 at 2.1 µm, respectively [25,26]. Both values were obtained with nanosecond pulses as the pump. Here the damage threshold is specified with femtosecond pulses at 2.4 µm by increasing the average power of the driving pulses until damage was observed, characterized by a sudden drop in transmitted power and the appearance of a visible damage hole on the front surface and cracks on the crystal. Two crystals were tested and both exhibited damage at 1.3 W, which corresponds to a peak intensity of approximately 40.5 GW/cm^2. The damage threshold is currently limited by the crystal quality, which can be improved further in the future according to the manufacturer.

3. Conclusion

In conclusion, we have demonstrated a MIR source with the BGSe crystal based on the IDFG method. A femtosecond Cr:ZnS laser system at the wavelength of 2.4 µm was used as the driving source, enabling a simultaneous spectral coverage from 6 to 18 µm. To the best of our knowledge, this is the first time broadband MIR generation has been realized in a BGSe crystal. The output is expected to have few-cycle pulse durations and also to be stable in its carrier-envelope phase. Compared to other crystals in Table 1, the preliminary result with BGSe shows a MIR generation with comparable broad bandwidth (wider than ZGP and LGS) although with a lower average power and conversion efficiency. Higher average power could be expected with further optimization of the focus spot size and crystal thickness. A better crystal quality with higher damage threshold would also be beneficial for increasing the MIR average power and conversion efficiency. This work shows that BGSe crystal is a promising material for the broadband, coherent MIR generation.

Funding

National Natural Science Foundation of China (No. 11974220).

Acknowledgments

We thank Prof. Ferenc Krausz for the great support and Dr. Alexander Kessel for providing the one-dimensional (1D) + time split-step simulation code.

Disclosures

The authors declare no conflicts of interest.

References

1. J. Haas and B. Mizaikoff, “Advances in mid-infrared spectroscopy for chemical analysis,” Annu. Rev. Anal. Chem. **9**(1), 45–68 (2016).
2. C. R. Petersen, U. Møller, I. Kubat, B. Zhou, S. Dupont, J. Ramsay, T. Benson, S. Sujecki, N. Abdel-Moneim, and Z. Tang, “Mid-infrared supercontinuum covering the 1.4–13.3 µm molecular fingerprint region using ultra-high NA chalcogenide step-index fibre,” Nat. Photonics **8**(11), 830–834 (2014).
3. T. Steinle, F. Neubrech, A. Steinmann, X. Yin, and H. Giessen, “Mid-infrared Fourier-transform spectroscopy with a high-brilliance tunable laser source: investigating sample areas down to 5 µm diameter,” Opt. Express **23**(9), 11105–11113 (2015).
4. H. J. Bakker and J. L. Skinner, “Vibrational spectroscopy as a probe of structure and dynamics in liquid water,” Chem. Rev. **110**(3), 1498–1517 (2010).
5. A. A. Lanin, A. A. Voronin, A. B. Fedotov, and A. M. Zheltikov, “Time-domain spectroscopy in the mid-infrared,” Sci. Rep. **4**(1), 6670 (2015).
6. H. Timmers, A. Kowligy, A. Lind, F. C. Cruz, N. Nader, M. Silfies, G. Ycas, T. K. Allison, P. G. Schunemann, and S. B. Papp, “Molecular fingerprinting with bright, broadband infrared frequency combs,” Optica **5**(6), 727–732 (2018).
7. I. Pupeza, M. Huber, M. Trubetskov, W. Schweinberger, S. A. Hussain, C. Hofer, K. Fritsch, M. Poetzlberger, L. Vamos, and E. Fill, “Field-resolved infrared spectroscopy of biological systems,” Nature **577**(7788), 52–59 (2020).
8. V. Smolski, S. Vasilyev, I. Moskalev, M. Mirov, Q. Ru, A. Muraviev, P. Schunemann, S. Mirov, V. Gapontsev, and K. Vodopyanov, “Half-Watt average power femtosecond source spanning 3–8 µm based on subharmonic generation in GaAs,” Appl. Phys. B **124**(6), 101 (2018).
9. J. Zhang, K. F. Mak, N. Nagl, M. Seidel, D. Bauer, D. Sutter, V. Pervak, F. Krausz, and O. Pronin, “Multi-mW, few-cycle mid-infrared continuum spanning from 500 to 2250 cm^{-1},” Light: Sci. Appl. **7**(2), 17180 (2018).
10. Q. Wang, J. Zhang, A. Kessel, N. Nagl, V. Pervak, O. Pronin, and K. F. Mak, “Broadband mid-infrared coverage (2–17 µm) with few-cycle pulses via cascaded parametric processes,” Opt. Lett. **44**(10), 2566–2569 (2019).
11. S. Vasilyev, I. S. Moskalev, V. O. Smolski, J. M. Peppers, M. Mirov, A. V. Muraviev, K. Zawilski, P. G. Schunemann, S. B. Mirov, and K. L. Vodopyanov, “Super-octave longwave mid-infrared coherent transients produced by optical rectification of few-cycle 2.5-µm pulses,” Optica **6**(1), 111–114 (2019).
12. C. Gaida, M. Gebhardt, T. Heuermann, F. Stutzki, C. Jauregui, J. Antonio-Lopez, A. Schülzgen, R. Amezcua-Correa, A. Tünnermann, and I. Pupeza, “Watt-scale super-octave mid-infrared intrapulse difference frequency generation,” Light: Sci. Appl. **7**(1), 94 (2018).

Optics EXPRESS

13. T. P. Butler, D. Gerz, C. Hofer, J. Xu, C. Gaida, T. Heuermann, M. Gebhardt, L. Vamos, W. Schweinberger, and J. A. Gessner, "Watt-scale 50-MHz source of single-cycle waveform-stable pulses in the molecular fingerprint region," Opt. Lett. **44**(7), 1730–1733 (2019).
14. I. Pupeza, D. Sánchez, J. Zhang, N. Lilienfein, M. Seidel, N. Karpowicz, T. Paasch-Colberg, I. Znakovskaya, M. Pescher, and W. Schweinberger, "High-power sub-two-cycle mid-infrared pulses at 100 MHz repetition rate," Nat. Photonics **9**(11), 721–724 (2015).
15. F. Keilmann and S. Amarie, "Mid-infrared frequency comb spanning an octave based on an Er fiber laser and difference-frequency generation," J. Infrared, Millimeter, Terahertz Waves **33**(5), 479–484 (2012).
16. Q. Wang, J. Zhang, N. Nagl, V. Pervak, F. Krausz, O. Pronin, and K. F. Mak, "Highly Efficient Broadband Mid-Infrared Generation (2.8–12.5 µm) Based on a Compact Cr: ZnS Laser," in *2019 Conference on Lasers and Electro-Optics Europe & European Quantum Electronics Conference (CLEO/Europe-EQEC)*, 2019, p. 1.
17. J. Zhang, K. Fritsch, Q. Wang, F. Krausz, K. F. Mak, and O. Pronin, "Intra-pulse difference-frequency generation of mid-infrared (2.7–20 µm) by random quasi-phase-matching," Opt. Lett. **44**(12), 2986–2989 (2019).
18. J. Yao, D. Mei, L. Bai, Z. Lin, W. Yin, P. Fu, and Y. Wu, "$BaGa_4Se_7$: a new congruent-melting IR nonlinear optical material," Inorg. Chem. **49**(20), 9212–9216 (2010).
19. J. Yao, W. Yin, K. Feng, X. Li, D. Mei, Q. Lu, Y. Ni, Z. Zhang, Z. Hu, and Y. Wu, "Growth and characterization of $BaGa_4Se_7$ crystal," J. Cryst. Growth **346**(1), 1–4 (2012).
20. M. C. Ohmer, R. Pandey, and B. H. Bairamov, "Emergence of chalcopyrites as nonlinear optical materials," MRS Bull. **23**(7), 16–22 (1998).
21. V. V. Badikov, D. V. Badikov, V. B. Laptev, K. V. Mitin, G. S. Shevyrdyaeva, N. I. Shchebetova, and V. Petrov, "Crystal growth and characterization of new quaternary chalcogenide nonlinear crystals for the mid-IR: $BaGa_2GeS_6$ and $BaGa_2GeSe_6$," Opt. Mater. Express **6**(9), 2933–2938 (2016).
22. U. Elu, L. Maidment, L. Vamos, T. Steinle, F. Haberstroh, V. Petrov, V. Badikov, D. Badikov, and J. Biegert, "Few-cycle mid-infrared pulses from $BaGa_2GeSe_6$," Opt. Lett. **45**(13), 3813–3815 (2020).
23. F. Yang, J. Yao, H. Xu, K. Feng, W. Yin, F. Li, J. Yang, S. Du, Q. Peng, and J. Zhang, "High efficiency and high peak power picosecond mid-infrared optical parametric amplifier based on $BaGa_4Se_7$ crystal," Opt. Lett. **38**(19), 3903–3905 (2013).
24. F. Yang, J. Yao, H. Xu, F. Zhang, N. Zhai, Z. Lin, N. Zong, Q. Peng, J. Zhang, and D. Cui, "Midinfrared optical parametric amplifier with 6.4–11 µm range based on $BaGa_4Se_7$," IEEE Photonics Technol. Lett. **27**(10), 1100–1103 (2015).
25. N. Y. Kostyukova, A. A. Boyko, V. Badikov, D. Badikov, G. Shevyrdyaeva, V. Panyutin, G. M. Marchev, D. B. Kolker, and V. Petrov, "Widely tunable in the mid-IR $BaGa_4Se_7$ optical parametric oscillator pumped at 1064 nm," Opt. Lett. **41**(15), 3667–3670 (2016).
26. J. Yuan, C. Li, B. Yao, J. Yao, X. Duan, Y. Li, Y. Shen, Y. Wu, Z. Cui, and T. Dai, "High power, tunable mid-infrared $BaGa_4Se_7$ optical parametric oscillator pumped by a 2.1 µm Ho: YAG laser," Opt. Express **24**(6), 6083–6087 (2016).
27. B. Zhao, Y. Chen, B. Yao, J. Yao, and X. Duan, "High-efficiency, tunable 8-9 µm $BaGa_4Se_7$ optical parametric oscillator pumped at 2.1 µm," Opt. Mater. Express **8**(11), 3332–3337 (2018).
28. G. Liu, Y. Chen, Z. Li, K. Yang, B. Yao, J. Yao, R. Wang, C. Yang, S. Mi, and T. Dai, "High-beam-quality 2.1 µm pumped mid-infrared type-II phase-matching $BaGa_4Se_7$ optical parametric oscillator with a $ZnGeP_2$ amplifier," Opt. Lett. **45**(13), 3805–3808 (2020).
29. A. A. Boyko, N. Y. Kostyukova, V. Badikov, D. Badikov, and V. Petrov, "Intracavity difference-frequency mixing of optical parametric oscillator signal and idler pulses in $BaGa_4Se_7$," Appl. Opt. **56**(10), 2783–2786 (2017).
30. Y. He, Y. Guo, D. Xu, Y. Wang, and J. Yao, "High energy and tunable mid-infrared source based on $BaGa_4Se_7$ crystal by single-pass difference-frequency generation," Opt. Express **27**(6), 9241–9249 (2019).
31. X. Luo, Z. Li, Y. Guo, J. Yao, and Y. Wu, "Recent progress on new infrared nonlinear optical materials with application prospect," J. Solid State Chem. **270**, 674–687 (2019).
32. N. Tolstik, E. Sorokin, and I. T. Sorokina, "Kerr-lens mode-locked Cr: ZnS laser," Opt. Lett. **38**(3), 299–301 (2013).
33. S. Vasilyev, M. Mirov, and V. Gapontsev, "Kerr-lens mode-locked femtosecond polycrystalline Cr^{2+}: ZnS and Cr^{2+}: ZnSe lasers," Opt. Express **22**(5), 5118–5123 (2014).
34. N. Nagl, S. Gröbmeyer, V. Pervak, F. Krausz, O. Pronin, and K. F. Mak, "Directly diode-pumped, Kerr-lens mode-locked, few-cycle Cr: ZnSe oscillator," Opt. Express **27**(17), 24445–24454 (2019).
35. M. N. Cizmeciyan, H. Cankaya, A. Kurt, and A. Sennaroglu, "Kerr-lens mode-locked femtosecond Cr^{2+}: ZnSe laser at 2420 nm," Opt. Lett. **34**(20), 3056–3058 (2009).
36. Y. Wang, T. T. Fernandez, N. Coluccelli, A. Gambetta, P. Laporta, and G. Galzerano, "47-fs Kerr-lens mode-locked Cr: ZnSe laser with high spectral purity," Opt. Express **25**(21), 25193–25200 (2017).
37. A. Kessel, S. A. Trushin, N. Karpowicz, C. Skrobol, S. Klingebiel, C. Wandt, and S. Karsch, "Generation of multi-octave spanning high-energy pulses by cascaded nonlinear processes in BBO," Opt. Express **24**(5), 5628–5637 (2016).